Published in 'Wear 260 (2006) 919–932'

Development of a Simple 'Temperature versus Sliding Speed' Wear Map for the Sliding Wear Behaviour of Dissimilar Metallic Interfaces

I.A. Inman[*a], S.R. Rose[b], P.K. Datta[b]

[a] *School of Engineering, Durham University, South Road, Durham, DH1 3LE, UK*
[b] *Advanced Materials Research Institute, Northumbria University, Newcastle upon Tyne, NE1 8ST, UK*

Abstract

The variation in wear behaviour during limited debris retention sliding wear of Nimonic 80A versus Stellite 6 (counterface) between room temperature and 750°C, at sliding speeds of 0.314, 0.654 and 0.905 $m.s^{-1}$, was investigated. At 0.314 $m.s^{-1}$, mild oxidational wear was observed at all temperatures, due to transfer and oxidation of Stellite 6-sourced debris to the Nimonic 80A and resultant separation of the Nimonic 80A and Stellite 6 wear surfaces. Between room temperature and 450°C, this debris mostly remained in the form of loose particles (with only limited compaction), whilst between 510°C and 750°C, the particles were compacted and sintered together to form a wear protective 'glaze' layer.

At 0.654 and 0.905 $m.s^{-1}$, mild oxidational wear due to transfer and oxidation of Stellite 6-sourced debris was only observed at room temperature and 270°C (also 390°C at 0.654 $m.s^{-1}$). At 390°C (450°C at 0.654 $m.s^{-1}$) and above, this oxide was completely absent and 'metal-to-metal' contact resulted in an intermediate temperature severe wear regime – losses in the form of ejected metallic debris were sourced almost completely from the Nimonic 80A. Oxide debris, this time sourced from the Nimonic 80A sample, did not reappear until 570°C (630°C at 0.654 $m.s^{-1}$), however, were insufficient to eliminate completely severe wear until 690°C and 750°C. At both 0.654 and 0.905 $m.s^{-1}$, the oxide now preventing severe wear at 690°C and 750°C tended not to form 'glaze' layers on the surface of the Nimonic 80A and instead supported continued high wear by abrasion. This abrasive action was attributed to the poor sintering characteristics of the Nimonic 80A-sourced oxide, in combination with the oxides' increased mobility and decreased residency.

The collected data were used to compose a simple wear map detailing the effects of sliding speed and temperature on the wear of Nimonic 80A slid against Stellite 6, at these speeds and temperatures of between room temperature and 750°C.

Keywords: high temperature wear, dissimilar materials, oxide 'glaze' layer, Stellite 6, Nimonic 80A, wear map

1. Introduction

In many situations, such as power generation, transport, materials processing and turbine engines, high temperature wear is a serious problem [1-6]. This is accentuated by faster rates of surface oxidation, loss of mechanical hardness and strength of contacting surfaces, and changes in adhesion between these surfaces caused by the joint action of temperature and tribological parameters. Efforts to prevent such wear have included use of thermally stable and oxidation resistant materials, coatings and preoxidised surfaces [1, 5-11]. However, the environmental conditions severely restrict the choice of materials and coatings that can be used [1-6].

An alternative method of generating wear resistant surfaces is to take advantage of some of the events accompanying high temperature wear, such as oxidation, debris generation and elemental transfer between the contacting surfaces [1-6, 12]. Under certain conditions of temperature, pressure and speed, these events lead to the formation of 'glazes' on the

* Corresponding author - *E-mail address:* i.a.inman@durham.ac.uk (I.A. Inman).

contacting surfaces that can enhance resistance to further wear [1-6, 12-21]. Although 'glaze' formation and the general issues relating to wear have been extensively studied [1-6, 12-21], it is still difficult to predict the conditions that promote 'glaze' formation.

Previous studies have concentrated on the sliding wear of Nimonic 80A versus Stellite 6 at 0.314 $m.s^{-1}$ and 750°C [1-4], including the structures of these glaze layers to establish more clearly their mechanisms of formation. However, other studies have shown that various combinations of load, sliding speed and temperature can have a dramatic effect on wear behaviour [22-28], particularly whether or not a protective 'glaze' can form. For example, Lancaster [22] observed a transition from severe wear (metal-to-metal contact and high wear losses) to mild wear (oxide preventing metal-to-metal contact and keeping wear to low levels) during the sliding of 60/40 brass against a tool steel. He also noted that there was an intermediate range of sliding speeds during which severe wear was observed, with mild wear being observed at speeds below and above this range. Also, Welsh [23, 24] observed, during 'like-on-like' wear of low carbon steels, similar transitions from mild wear at low loads to severe wear at intermediate loads and mild wear at high loads. Increasing temperature or sliding speed could decrease the loads at which these transitions occurred. Also, So [27] noted the existence of mild to severe wear transition on increasing load during the sliding of Stellite versus martensitic steels.

Wear maps can be used to present wear data in an easy to understand manner that allows prediction of the likely mode of wear under certain sliding conditions. While Lim [29, 30] and Childs [31] designed wear maps based on load and sliding speed, other wear combinations can be used – for example, Kato and Hokkirigawa [32] opted for an abrasive wear map, using 'degree of penetration (of asperities)' and 'shear strength at the contact interface' as the key parameters. However, most wear maps have been constructed under room temperature conditions – few have involved sliding at high ambient temperature or on the effects of dissimilar interfaces.

It has been shown previously [1,4] that, for sliding Nimonic 80A against a counterface of Stellite 6, sliding speed and temperature can affect which surface undergoes the greater wear. The current paper expands on this previous work and considers in more detail the effects of sliding speed (from 0.314 $m.s^{-1}$ to 0.905 $m.s^{-1}$) and temperature (from room temperature to 750°C) on the same sample / counterface combination. The data were then used to construct a wear map based on sliding speed and temperature.

2. Experimental

The compositions of the alloys are detailed in Table 1.

	Fe	Ni	Cr	Al	Ti	Mn	W	Co	Si	C
Nimonic 80A	0.7	75.8	19.4	1.4	2.5	-	-	-	0.1	0.08
Stellite 6	2.5 max	2.5 max	27	-	-	1	5	60	1	1

Table 1: Nominal compositions of alloys (at%)

The tests were carried out on a high temperature 'reciprocating-block-on-rotating-cylinder' wear rig (the blocks forming the samples and the cylinder being the counterface) in air (Fig. 1). The configuration used was such that debris retention was not encouraged. The counterface (Stellite 6), diameter 50 mm and length 50 mm, was mounted on a shaft that was rotated by a variable speed electric motor. Cleaned samples of Nimonic 80A, 5 mm x 5 mm x 45 mm, polished to a 1 µm surface finish, were held against the cleaned counterface (polished to a 1200 grit finish) using a sample arm in reciprocating motion at 3 cycles per minute and a constant stroke of 12 mm. The tests were carried out at speeds of 0.314 $m.s^{-1}$, 0.654 $m.s^{-1}$ and 0.905 $m.s^{-1}$, under a load of 7 N at temperatures between room temperature and 750°C. The total sliding distance for all tests was 4,522 m.

A minimum of three tests (one per sample) was conducted for each combination of conditions. Each sample of Nimonic 80A was weighed using a high accuracy Sartorious microbalance before and after sliding, from which a mean weight change for each combination was calculated. The wear of the Stellite 6 counterface was not assessed quantitatively as discussed elsewhere [1]. The friction data were collected by a Melbourne type TRP-50 torque transducer, connected to the rotating counterface shaft.

The wear surfaces were characterised at a micro-scale level as described previously [1-6]. The microstructures were characterised using scanning electron microscopy (SEM), energy dispersive X-ray (EDX) and X-ray diffraction analysis (XRD). The weight change and characterisation data were used to construct a simple wear map for this combination, based on the nature of the wear observed for different combinations of temperature and sliding speed.

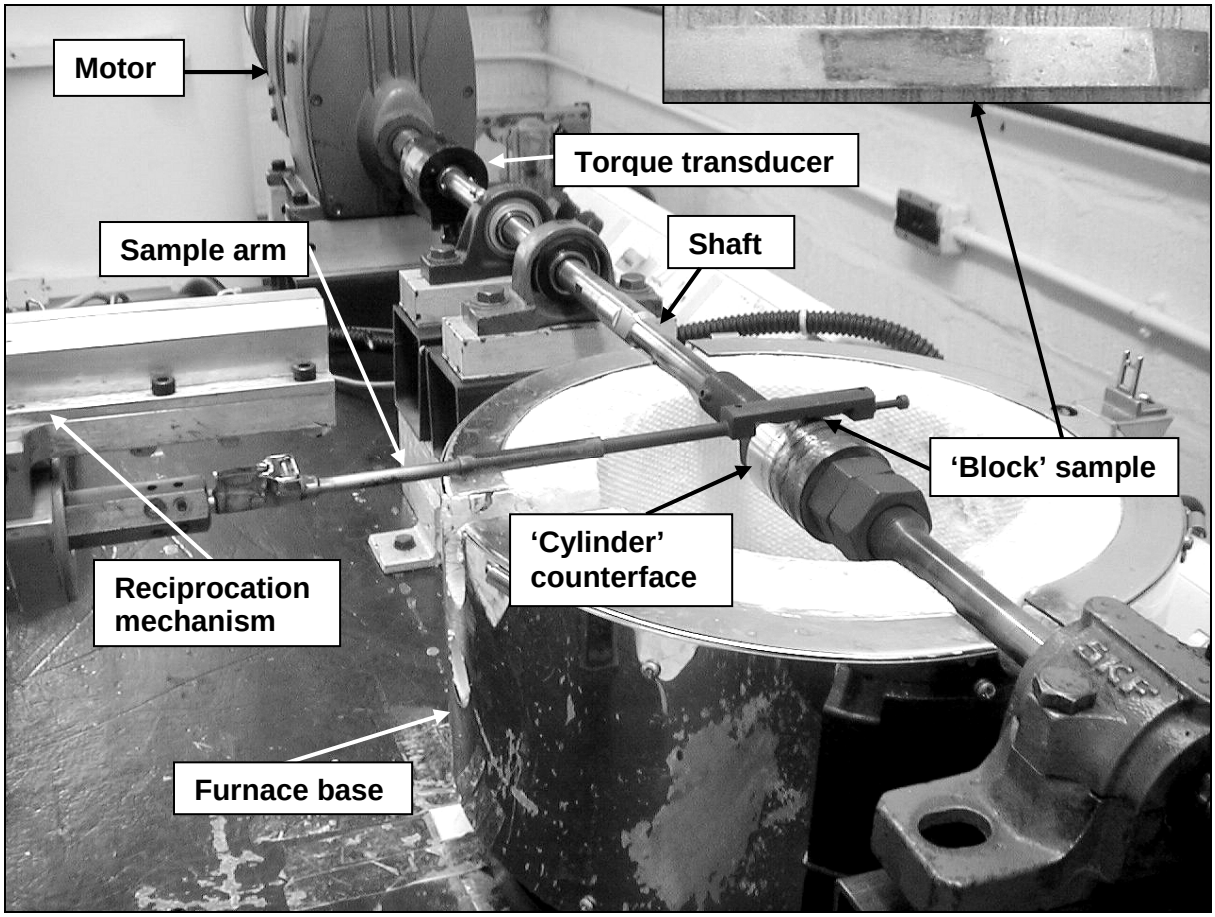

Fig. 1: Reciprocating high temperature block-on-cylinder wear rig plus a Nimonic 80A 'block' sample (shown example with 'glaze' layer formed by sliding at 0.314 $m.s^{-1}$ and 750°C against a Stellite 6 counterface or 'cylinder' – load 7N, sliding distance 4,522 m)

3. Results

3.1. Wear at 0.314 $m.s^{-1}$

Following testing at 0.314 $m.s^{-1}$, the Nimonic 80A sample weight change values were extremely low for all temperatures (Fig. 2) due to the rapid formation of loose debris between room temperature and 450°C, and comprehensive 'glaze' layers between 510°C and 750°C (Fig. 3).

Very slight weight losses were recorded at room temperature with a negligible weight loss observed at 390°C (Fig. 2). These losses coincided with the presence of fine loose oxide debris (300 nm to 1 µm) and some areas of compacted oxide on the wear scar surfaces of both the sample (Fig. 3) and the counterface (not shown). At 390°C, some sintering of the debris particles was observed. A very slight weight gain at 450°C coincided with further evidence of particle sintering and also the appearance of isolated patches of 'glaze', although most oxide remained in the form of loose debris. EDX analysis indicated that the fine oxide debris contained varying amounts of Ni, Cr and Co; some location to location variation was

observed. In an area rich in oxide particles, such analyses indicated up to 50% Co and up to 60% Ni (60% Ni being coincident with Co levels of less than 10%). In areas relatively free of particles, the analyses consistently indicated a high level of Ni (up to 60%) and no Co, suggesting no transfer of metal between the counterface and the sample. The usually high levels of Co and Cr and low levels of Ni in the oxide particles indicate that debris generation was normally dominated by material transferred from the Stellite 6 counterface. At 450°C, EDX indicated consistently high levels of Co (up to 50%) as wear scar debris coverage increased.

Weight gains were observed for Nimonic 80A at temperatures between 510°C and 750°C, apart from 570°C where a weight loss was recorded. This last result was reproduced in 8 tests suggesting that the wear process needs further attention at this temperature (Fig. 2). The weight gains coincided with the formation of more extensive 'glaze' layers on the wear scar surfaces of both the sample (Fig. 3) and the counterface (not shown). Moderate quantities of loose debris were present on the sample at 510°C; however, between 570°C and 750°C, very little loose debris was observed; most was incorporated into the 'glaze' layers.

The comprehensive formation of 'glaze' layers from 510°C upwards coincided with increasing Co levels in the 'glaze'-covered regions, although the levels were fairly variable, between 35 and 55 %. The levels of Ni dropped to less than 10% within the 'glaze', although some spot analyses gave between 15 and 18%, particularly at 570°C, where 'glaze' coverage was incomplete (thus the data may have been affected by the Nimonic 80A substrate) and at 750°C, where standard analyses indicated more general Ni levels of 18%, with some location-to-location variation. Cr levels in the 'glaze' were consistently 30 to 35%. The high levels of Co and Cr indicate that most of the oxide forming the 'glaze' was sourced from the counterface. The very low levels of Ni indicate only a limited contribution from the Nimonic 80A sample.

XRD analysis at all temperatures indicated the presence of one or more of Cr_2O_3, $CoCr_2O_4$ and Co_3O_4 (all have near-identical diffraction patterns) in the 'glaze' layers, with $CoCr_2O_4$ and Co_3O_4 as the dominant phases. The Nimonic 80A gave a face-centred-cubic Ni-Cr-Fe phase.

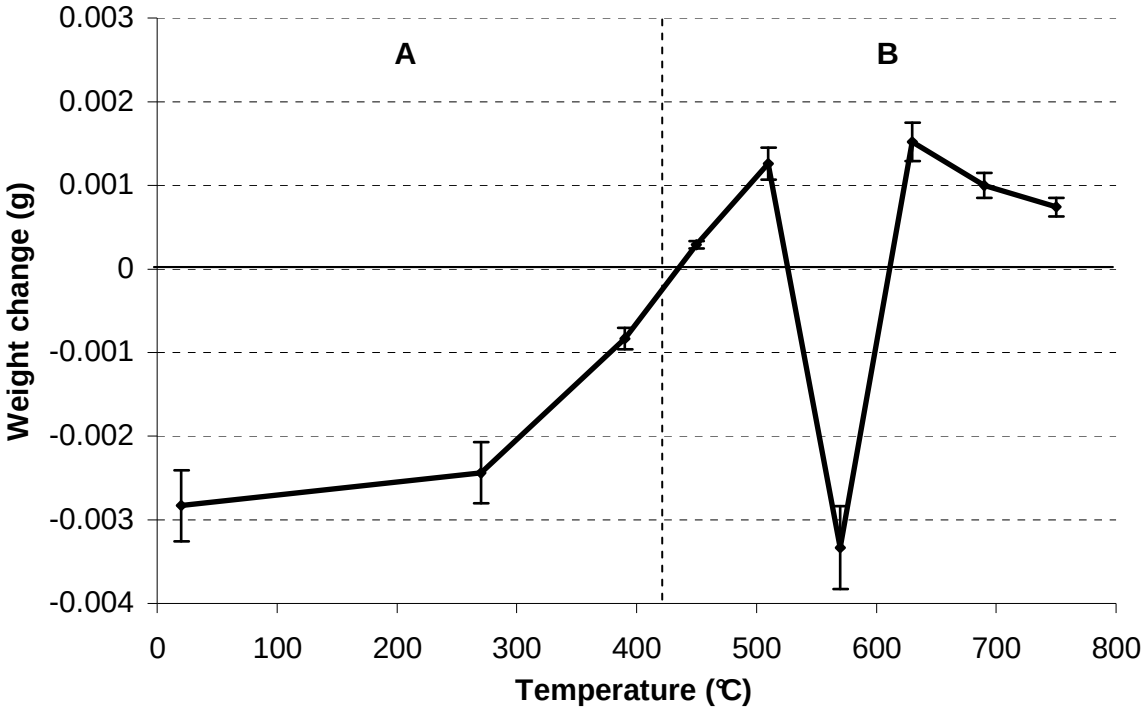

A. Loose oxide debris spread across wear surface, plus some compacted oxide formation (room temperature to 390℃) and isolated 'glaze' fo rmation (450℃ only)
B. Smooth 'glaze' layers with only a little loose debris (510℃ to 750℃)
(Representative micrographs shown in Fig. 3)

Fig. 2: Weight change versus temperature for Nimonic 80A slid against Stellite 6 at 0.314 $m.s^{-1}$ (load 7N, sliding distance 4,522 m)

The friction versus time plots (Fig. 4) showed an initial unsettled period before, in many cases, settling into a 'steady state' period with less variation. In addition, there was a clear downward trend of friction with temperature, both for peak values during the 'run-in' period and during the later 'steady state' period. Values during the unsettled period rose from zero to 1.14 at room temperature, 0.78 at 270°C, 0.7 at 510°C and 0.63 at 750°C. Typical steady state values were ~0.8 at room temperature, 0.7 to 0.8 at 270°C, 0.6 to 0.7 at 510°C and ~0.5 at 750°C, with any variation being no more than approximately 12% of the mean value. The very brief run-in period at 750°C indicates that the onset of 'glaze' layer formation was almost immediate and the steady state friction values after this initial peak were due to the continued presence of 'glaze' on the wear surfaces.

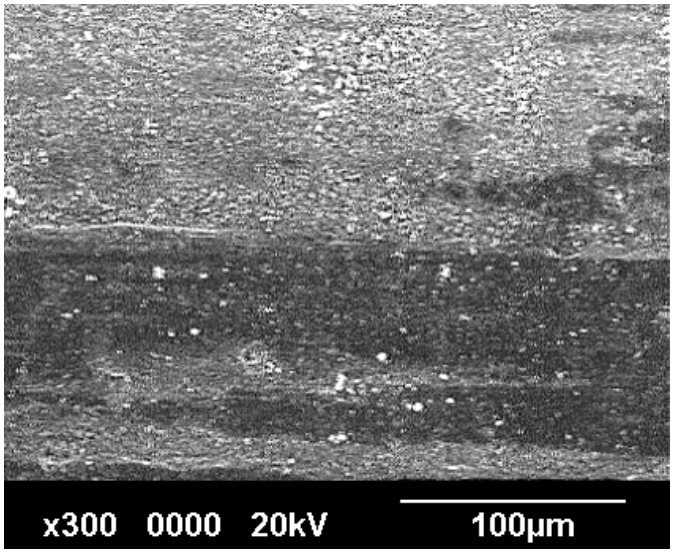	*A. Room temperature (shown), also typical of 270, 390 and 450℃*
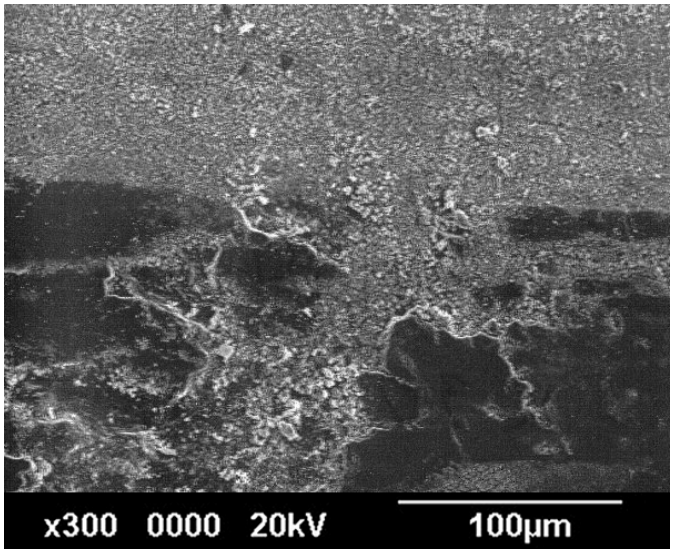	*B. 510℃*
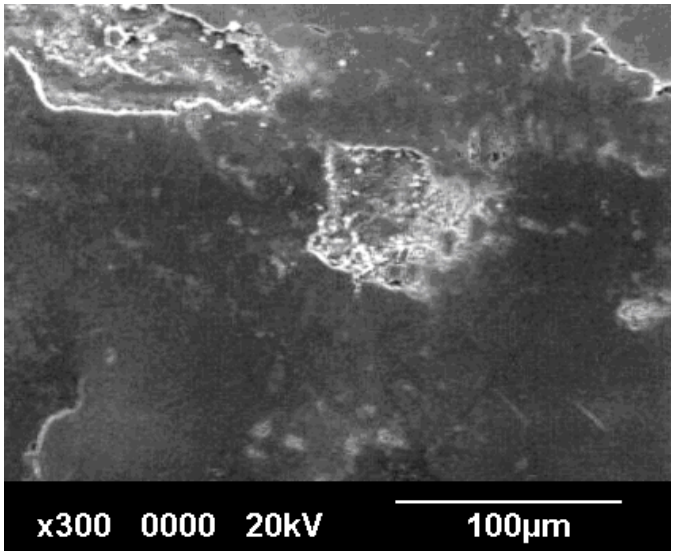	*C. 750℃ (shown), also typical of 570, 630 and 690℃*

Fig. 3: SEM micrographs of Nimonic 80A wear surfaces after sliding at 0.314 $m.s^{-1}$ (load 7N, sliding distance 4,522 m) against a Stellite 6 counterface at room temperature, 510 and 750°C

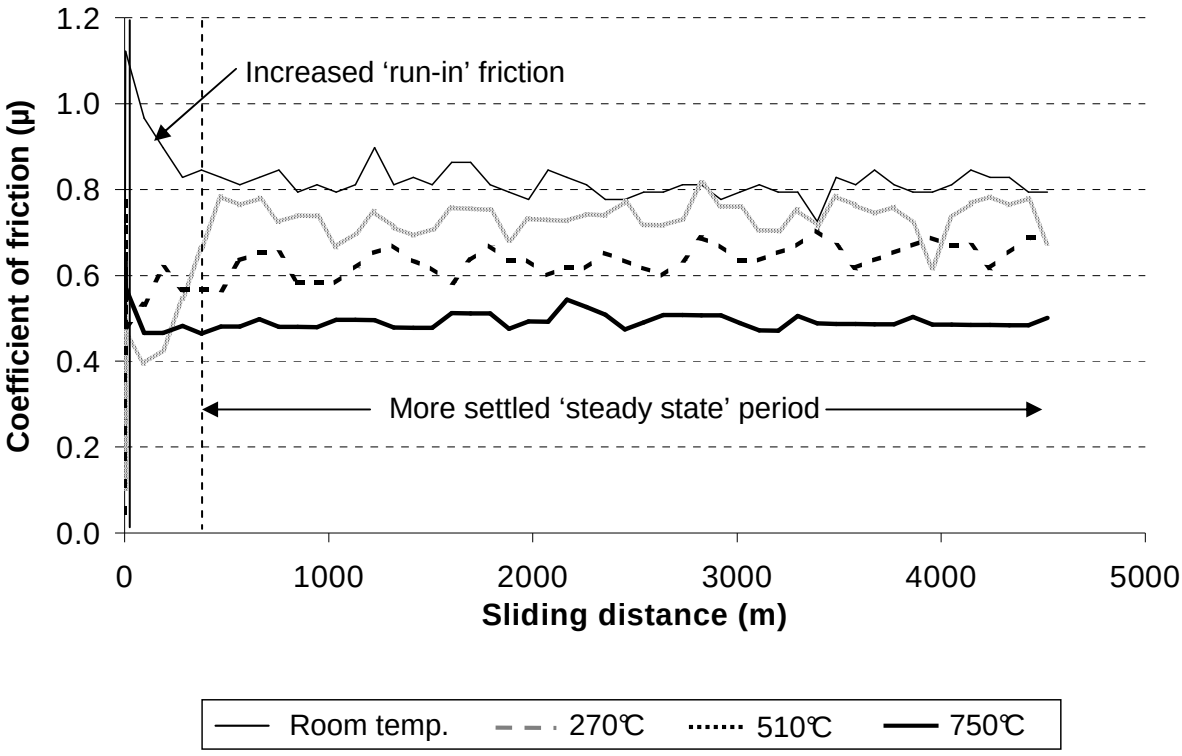

Fig. 4: Representative coefficient of friction versus sliding distance plots for Nimonic 80A versus Stellite 6 at 0.314 $m.s^{-1}$ (load 7N, sliding distance 4,522 m)

3.2 Wear at 0.654 $m.s^{-1}$

During sliding at 0.654 $m.s^{-1}$, the wear losses were low at room temperature, 270°C and 390°C (Fig. 5), coinciding with the presence of very fine loose oxide debris (300 nm to 1 μm) and a few isolated areas of compacted oxide on both the sample and the counterface surfaces (Fig. 8). As at 0.314 $m.s^{-1}$, such debris prevented metal-to-metal contact and severe wear by metallic adhesion [1]. Some deformation and smearing (onto the wear surfaces) of these particles was observed at 270°C and, especially, at 390°C. Examination and analyses of the sample surfaces gave similar results to those formed at 0.314 $m.s^{-1}$, with areas high in fine particle debris showing high Co levels (up to ~55%), indicating transfer from the Stellite 6 counterface, and areas relatively free of particles giving higher Ni levels (up to 60%) from the underlying Nimonic 80A sample. XRD, combined with EDX, analysis of debris-rich surfaces indicated one or more of Cr_2O_3, $CoCr_2O_4$ and Co_3O_4. A face-centred-cubic Ni-Cr-Fe pattern was also detected, typical of Nimonic 80A.

A transition was observed in the weight change data at 450ºC, to a higher weight loss, consistent with a severe 'metal-against-metal' wear regime symptomatic of adhesive wear

[1]. This was accompanied by large volumes of metallic debris and bright, highly damaged metallic wear surfaces on both the sample (Fig. 8) and the counterface (not shown).

This high loss, metallic wear regime also dominated at higher temperatures and the weight losses increased. Oxide was completely absent from the sample and counterface wear surfaces at 450ºC, 510ºC and 570ºC, although, at 630ºC, a limited amount of oxide was observed. However, the oxide debris at 630ºC was insufficient to prevent metal-to-metal contact and metallic severe wear continued. The debris was readily ejected from the surfaces and there were no signs of glaze layer formation on either sample or counterface surfaces.

Between 450ºC and 630ºC, EDX analysis indicated a composition typical of Nimonic 80A (~70% Ni, ~25% Cr) for both the ejected metallic debris and the exposed metallic surface of the wear scar. Co levels were almost negligible, showing no material transfer (metallic or oxide) from the counterface. XRD analysis only revealed the Ni-Cr-Fe phase typical the Nimonic 80A. EDX analysis of the limited oxide debris generated at 630ºC also indicated high levels of Ni and Cr, sourced from the Nimonic 80A (~69% Ni, ~26% Cr). There was insufficient oxide debris to allow XRD analysis.

A further wear transition to a high temperature oxidational wear regime was observed at 690°C and 750°C – this coincided with decreases in the weight loss due to wear (Fig. 5). However, the data at 690°C and 750°C also indicate that, despite these decreases, overall, wear still remained high. This wear regime was characterised by high levels of oxide debris generation and a smooth but heavily worn sample wear surface across which fine straight grooves, parallel to the direction of sliding, were covered by only a very thinly smeared layer of oxide (Fig. 8). These grooves indicated that the primary action of the oxide debris was abrasion and, hence, material removal and wear remained high. Whilst the high levels of oxide debris did prevent metal-to-metal contact and, thus, severe wear, the oxides showed no tendency to develop into either compacted oxide or ‘glaze’ layers. However, on the counterface there was a more substantial, but still limited, development of ‘glaze’ layers, accompanied by a decrease in counterface wear damage (not shown).

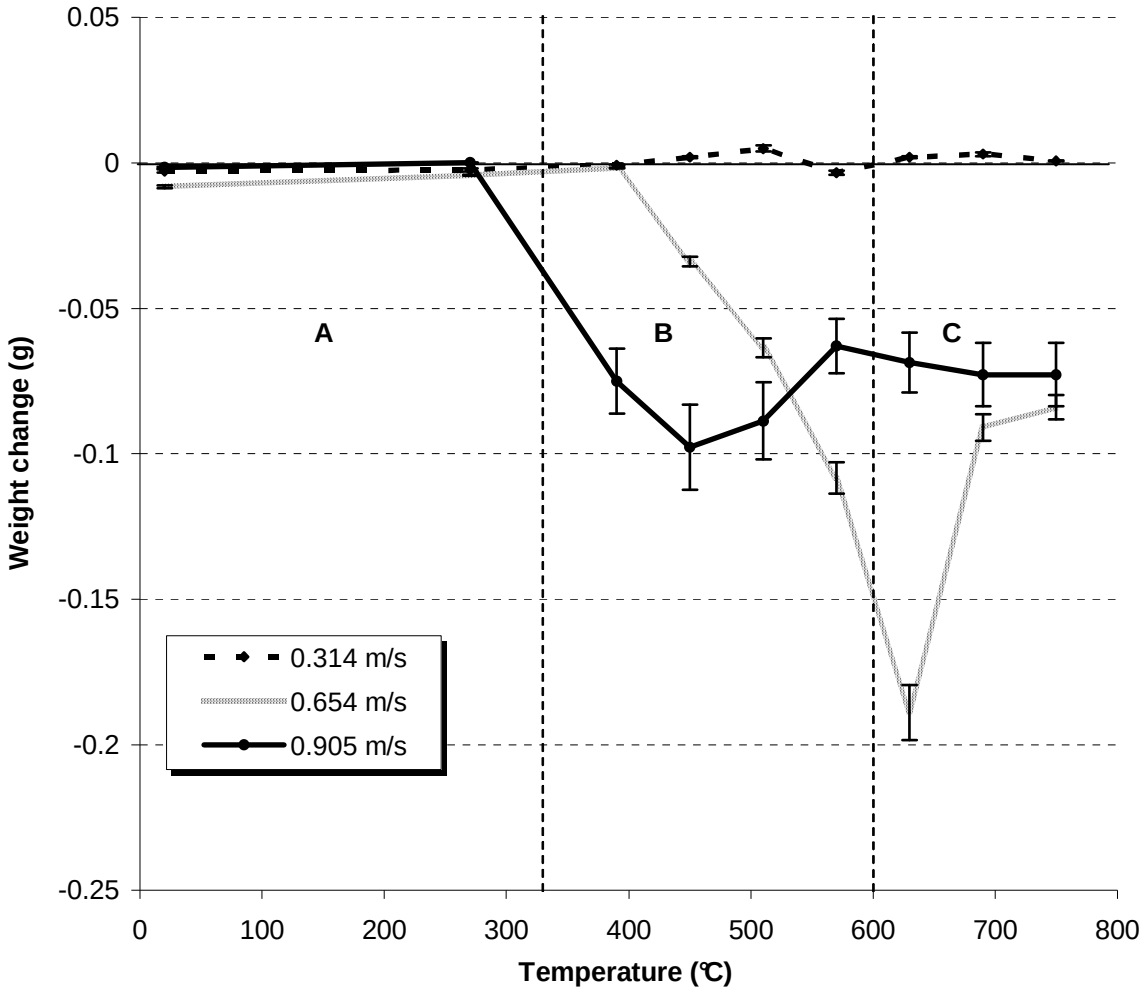

A. Loose oxide debris spread across wear surface, plus some compacted oxide formation (room temperature and 270℃ at both 0.654 m.s^{-1} and 0.905 m.s^{-1}, also 390℃ at 0.654 m.s^{-1})

B. Torn, metallic surface typical of adhesive wear, no traces of any oxide debris (390℃ to 510℃) or only very limited oxide debris formation (at 0.905 m.s^{-1} – 570℃; at 0.654 m.s^{-1} and 0.905 m.s^{-1} – 630℃)

C. Loose oxide but with no compact oxide layers at 0.654 m.s^{-1} and only isolated build-ups of oxide at 0.905 m.s^{-1}; fine parallel grooves in direction of sliding on Nimonic 80A surface (690℃ to 750℃)

Micrographs shown in Figs. 6 and 8

Fig. 5: Weight change versus temperature for Nimonic 80A slid against Stellite 6 at 0.654 m.s^{-1} and 0.905 m.s^{-1} (load 7N, sliding distance 4,522 m) – data for 0.314 m.s^{-1} also shown

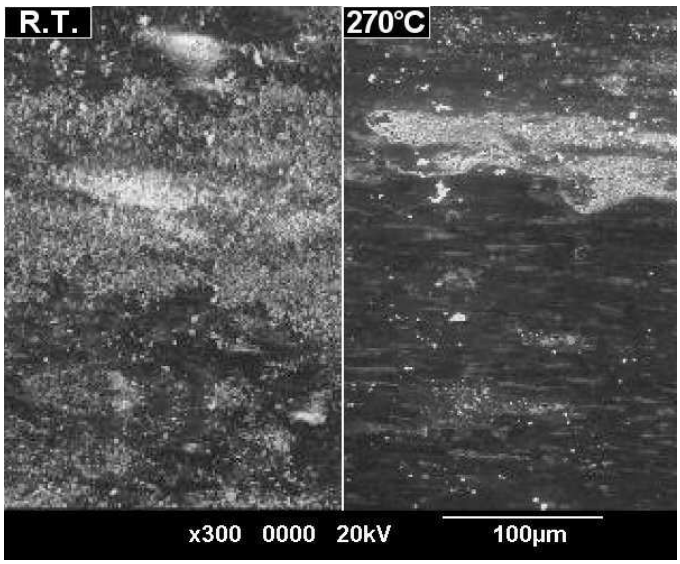

A. Room temperature and 270℃ (shown), also typical of 390ºC

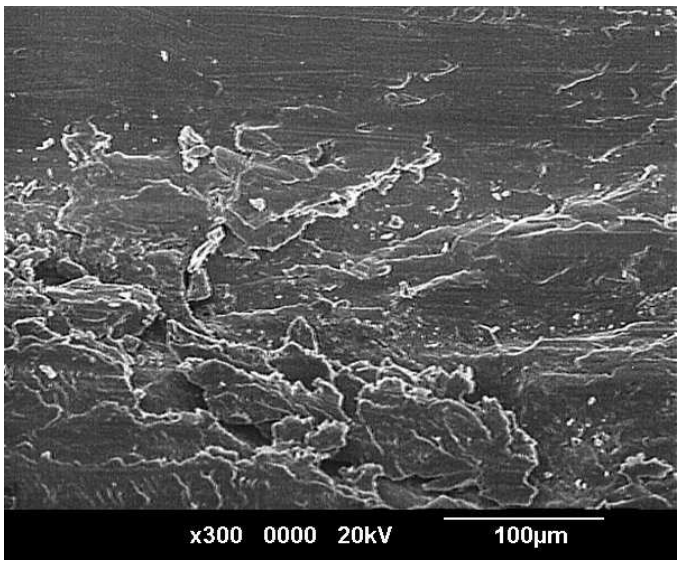

B. 570℃ (shown), also typical of 450, 510 and 630℃

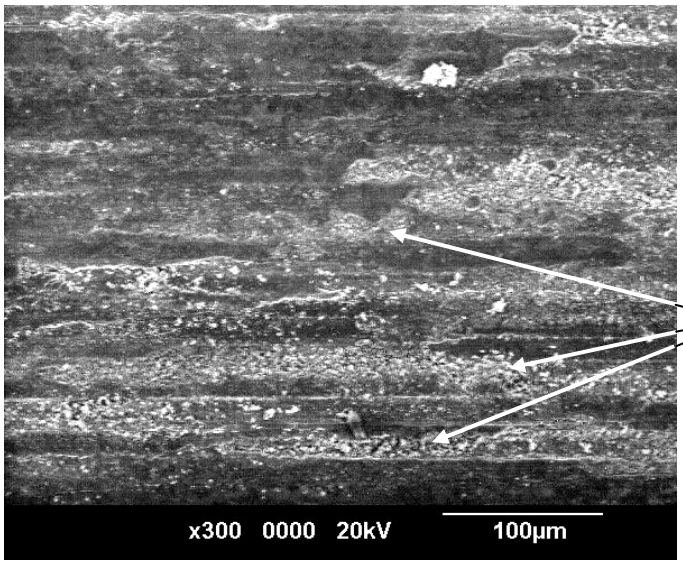

C. 750℃ (shown), also typical of 690℃

Parallel grooves due to abrasion (holding some loose oxide debris)

Fig. 6: SEM micrographs of Nimonic 80A wear surfaces after sliding at 0.654 $m.s^{-1}$ (load 7N, sliding distance 4,522 m) against a Stellite 6 counterface at room temperature, 270, 570 and 750°C

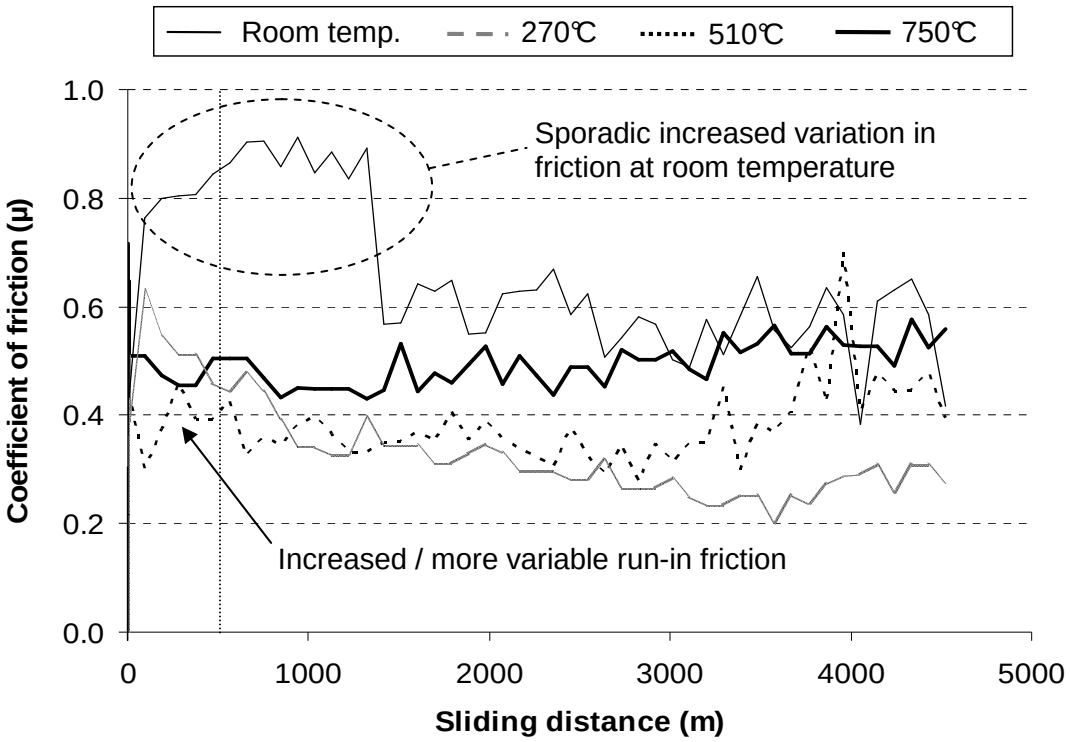

(a) 0.654 m.s^{-1}

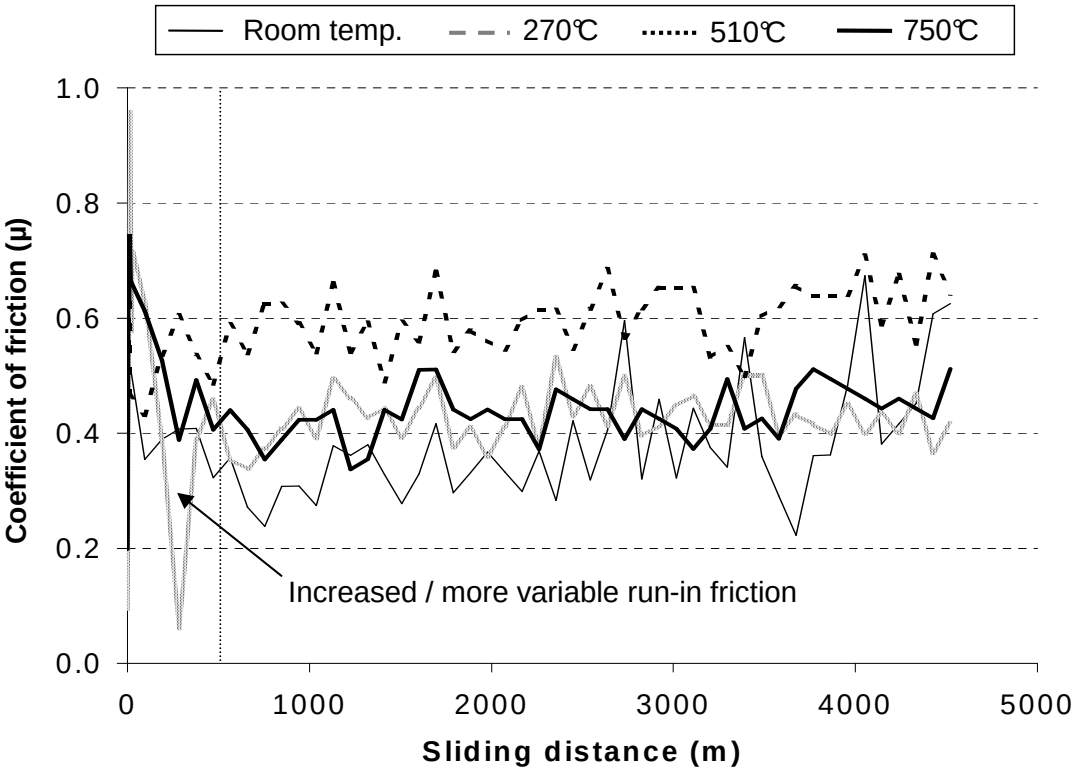

(b) 0.905 m.s^{-1}

Fig. 7: Representative coefficient of friction versus sliding distance plots for Nimonic 80A versus Stellite 6 at room temperature, 270ºC, 510ºC and 750ºC, for sliding speeds of (a) 0.654 m.s^{-1} and (b) 0.905 m.s^{-1} (load 7N, sliding distance 4,522 m)

The fine, thinly smeared oxide layer on the sample surfaces at 690ºC and 750°C had no effect on the EDX analysis. Both the thinly smeared layer of oxide on the sample and the loose oxide debris gave compositions of ~71% Ni and ~25% Cr (similar to that of the Nimonic 80A). No significant Co could be detected to suggest material transfer from the counterface. Oxide from the limited 'glaze' layers on the counterface gave similar results (~68% Ni, ~25% Cr) to the loose debris, indicating that 'glaze' had formed from the debris. The dominant phases indicated by XRD of the sample were a Ni-Cr-Fe phase from the Nimonic 80A, and a very weak signal for NiO from the very thinly smeared oxide layer. Moreover, NiO and Cr_2O_3 were detected in the copious loose debris.

The representative friction values at 0.654 $m.s^{-1}$ (Fig. 7) indicated an initial unsettled period, followed by in many cases a 'steady state' with less variation. However, unlike 0.314 $m.s^{-1}$, there was no visible trend relating friction to temperature. The values during the unsettled period rose from zero to 0.91 at room temperature, 0.72 at 270°C, 0.50 at 510°C and 0.64 at 750°C. The onset of steady state sliding (normally within 500 m of the start) saw values generally between 0.38 and 0.66 at room temperature, 0.20 and 0.40 at 270°C, 0.30 and 0.50 at 510°C and 0.45 and 0.58 at 750°C. During steady state, the variation in friction was within a 15% band up to 630ºC, compared to 12% at 0.314 $m.s^{-1}$, regardless of whether there was direct metal-to-metal contact or oxide was present on the wear surfaces. The variation dropped to ~12% at 690ºC and 750ºC, coinciding with high levels of NiO and Cr_2O_3 debris from the Nimonic 80A and limited formation of 'glaze' on the counterface. Here, the switch to steady state occurred very rapidly, within the first 300 m of sliding.

3.3 Wear at 0.905 $m.s^{-1}$

The data for 0.905 $m.s^{-1}$ indicate a similar wear profile to that at 0.654 $m.s^{-1}$. However, some temperature-influenced differences (notably in transition temperatures between modes of wear) were observed. Weight losses (Fig. 5) remained low at room temperature and 270°C; this coincided with the presence of very fine loose oxide (300 nm to 1 µm) and some isolated areas of compacted oxide on both the sample (Fig. 8) and the counterface wear surfaces. The loose oxide debris prevented metal-to-metal contact and severe wear by metallic adhesion [1]. Some deformation and smearing of debris particles (onto wear surfaces) was observed at 270°C. The EDX and XRD data were similar to those for 0.314 $m.s^{-1}$ and also up to 390°C at 0.654 $m.s^{-1}$ (i.e. conditions for which loose debris was observed); areas with copious debris were Co-rich and areas devoid of debris were high Ni from the underlying sample.

Higher test temperatures resulted in a transition to a high weight loss severe 'metal-to-metal' wear regime (for both the sample and counterface surfaces) symptomatic of adhesive wear [1], as was the case at 0.654 $m.s^{-1}$. However, at 0.905 $m.s^{-1}$, this transition was observed at 390°C, compared to 450°C at 0.654 $m.s^{-1}$ (Fig. 5). This severe 'metal-to-metal' wear regime continued at 450°C, 510°C, 570°C and 630°C. At 390°C, 450°C and 510°C, the debris generated was metallic in nature and no debris, metallic or oxide, was retained at the wear interface – at these temperatures, wear was higher than at 0.654 $m.s^{-1}$ (Fig. 5). Limited oxide debris generation was only observed at 570°C, at levels insufficient to prevent metal-to-metal contact and severe wear continued. At 630°C, the amount of oxide debris increased and sufficient oxide was collected to allow XRD to identify a mixture of NiO and Cr_2O_3 (EDX indicated ~70% Ni, 24% Cr). However, a severe 'metal-to-metal' wear regime continued to dominate at 570°C and 630°C, despite the presence of this oxide (though a little oxide was observed on the counterface at 630°C).

Between 390°C and 570°C, EDX analysis indicated a high Ni-Cr content (~70% Ni, 25% Cr), while Co levels remained almost negligible, showing no material transfer from the counterface; there was also no Co in the ejected metallic debris.

A further wear transition was observed at 690°C to a high temperature oxidational wear regime (very similar to that observed at 0.654 $m.s^{-1}$), with continued high weight losses. This regime was characterised by high levels of oxide debris and a smooth, though still heavily worn, sample wear surface, covered by a very thinly smeared layer of oxide (Fig. 8). The formation of fine, straight grooves parallel to the direction of sliding indicated that the increase in sliding speed from 0.654 $m.s^{-1}$ to 0.905 $m.s^{-1}$ did not significantly change the role of the oxide debris in acting as an abrasive agent and, hence, wear remained high. This regime was also observed at 750°C.

Losses due to wear at 0.905 $m.s^{-1}$ were lower at 690°C and 750°C than at 0.654 $m.s^{-1}$ (Fig. 5); these coincide with more pronounced oxide generation and higher levels of loose debris on the sample surfaces (Fig. 6 and Fig. 7). The debris once again showed little tendency to form into either compacted oxide or 'glaze' layers, though SEM did indicate some very limited oxide build-up in isolated patches. Only on the counterface was there limited build-up of more highly developed but still patchy 'glaze' layers, accompanied by a decrease in wear-related damage (not shown).

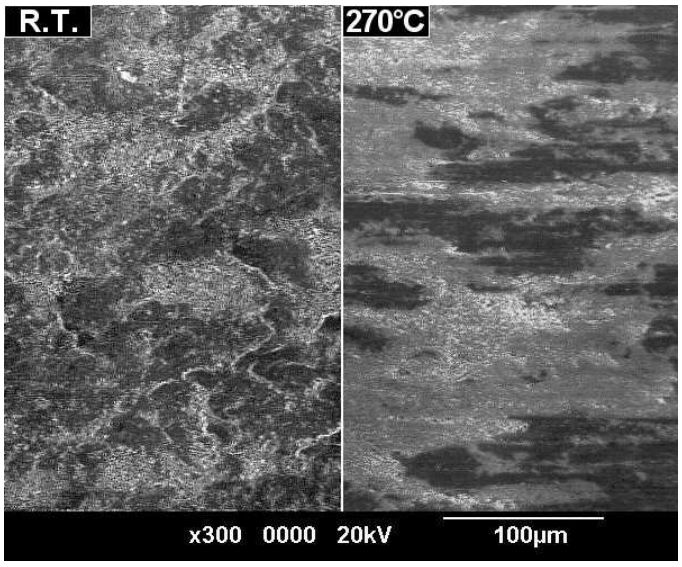

A. Room temperature and 270℃

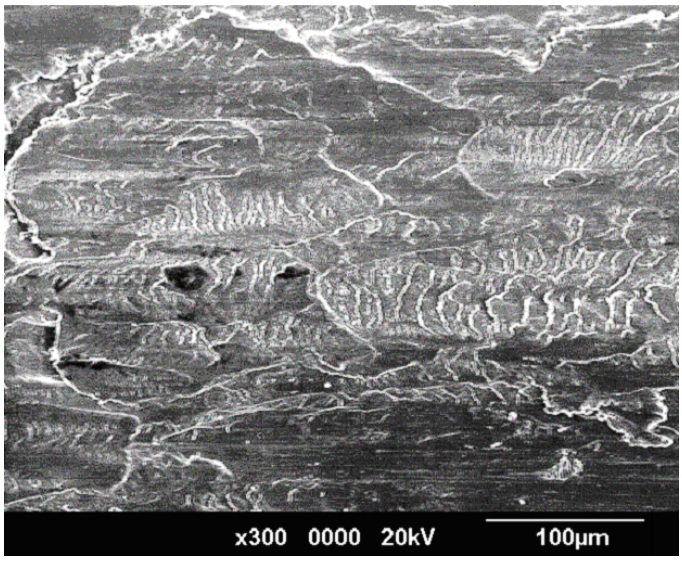

B. 390℃ (shown), also typical of 450, 510, 570 and 630℃

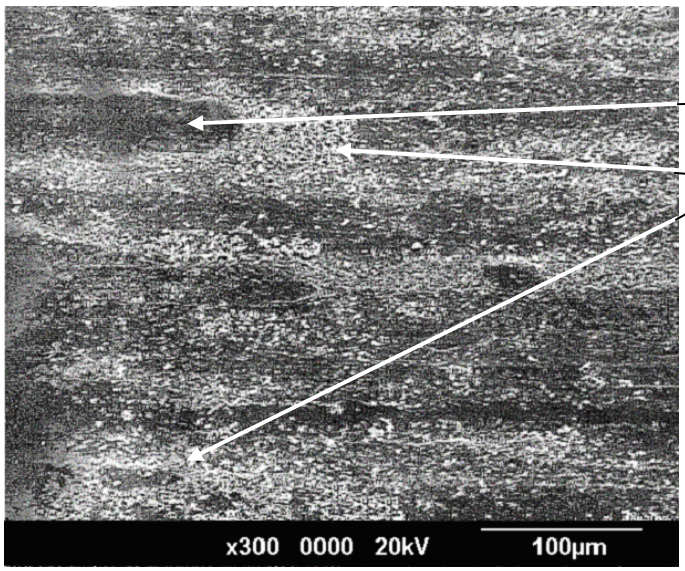

Limited oxide build-up

Loose oxide

C. 750℃ (shown), also typical of 690℃

Fig. 8: SEM micrographs of Nimonic 80A wear surfaces after sliding at 0.905 $m.s^{-1}$ (load 7N, sliding distance 4,522 m) against a Stellite 6 counterface at room temperature, 270, 390 and 750°C

The appearance of the very fine, thinly smeared oxide layer on the samples from 630ºC upwards had no effect on the EDX analysis. Both the thinly smeared layer of oxide on the sample (including the isolated patches of oxide) and the high levels of loose oxide debris gave a composition of ~71% Ni and ~24% Cr, with again no significant Co. Oxide removed from the limited 'glaze' layers formed on the Stellite 6 counterface at 690ºC and 750ºC gave similar results to the debris – the limited 'glaze' layers were oxide debris generated from the Nimonic 80A sample, as at 0.654 $m.s^{-1}$. The dominant phases identified by XRD were a very weak signal for NiO (from the very thinly smeared oxide layer) and a Ni-Cr-Fe phase typical of Nimonic 80A. With no Co in the copious amounts of loose debris, XRD indicated the dominance of NiO and Cr_2O_3.

The representative friction values (Fig. 7) showed an early unsettled period, before a 'steady state' with lesser variation. However, as at 0.654 $m.s^{-1}$ and unlike 0.314 $m.s^{-1}$, there was no visible trend of friction values with temperature.

Values of friction during the unsettled period rose from zero to 0.53 at room temperature, 0.95 at 270°C, 0.72 at 510°C and 0.73 at 750°C. On achieving steady state (within 500 m), values settled to between 0.23 and 0.60 at room temperature, 0.35 and 0.50 at 270°C, 0.48 and 0.68 at 510°C and 0.35 and 0.50 at 750°C; no temperature related trends were observed. The variation in friction during steady state was within a 20% band between room temperature and 630ºC though could occasionally rise to as great as 50% at room temperature and at 270°C; this was regardless of whether or not oxide was present on the wear surfaces and able to prevent metal-to-metal contact. Variation levels dropped to ~15% at 690ºC and 750ºC, coinciding with the generation of high levels of NiO and Cr_2O_3 debris and limited formation of 'glaze' on the counterface. At 690ºC and 750ºC (Fig. 7), the switch from run-in to steady state friction occurred rapidly, within the first 300 m of sliding.

4. Discussion

4.1 Sliding at 0.314 $m.s^{-1}$

The formation of oxides and their subsequent transformation to 'glaze' with increasing sliding distance and temperature significantly influenced the wear behaviour at this speed.

The observed rapid formation of oxide particles that separated the sliding surfaces was responsible for the low wear, even at room temperature and 270°C where 'glaze' was not developed. Here, the oxides predominantly resided on the Nimonic 80A surface as patches

of loose particles; the agglomeration of the particles increased with increasing sliding distance and temperature. The analyses of the debris suggest that the low levels of wear observed occurred predominantly on the Stellite 6 surface.

As the temperature increased the nature of the oxide deposits changed. The loose particles underwent agglomeration and sintering at 390^{o}C, with the onset of 'glaze' formation at 450^{o}C. The coverage of the surface by 'glaze' increased with temperature, with comprehensive layers at temperatures between 510°C and 750^{o}C. Once such 'glaze' was formed, the wear substantially decreased. These 'glazes' are nano-crystalline in nature – their formation and characterisation are discussed in detail elsewhere [1-4].

Although it is difficult to ascertain the precise role of the chemical elements in the formation of 'glaze', the fully developed 'glaze' (at 750^{o}C) contained 60% Co and 30% Cr, due to both Co_3O_4 and $CoCr_2O_4$ (as shown by XRD analysis). One important observation is the initial preferential wear of the harder Stellite 6 compared to the extremely limited wear of the softer Nimonic 80A (Fig. 2). This was originally thought to be caused by a delamination type of mechanism due to probable low fatigue crack growth resistance and K_{Ic} value of Stellite 6 [1, 4]; however, recent data [33, 34] suggests that Stellite 6 has a high K_{Ic} value compared to nickel-based alloys. Thus, why Stellite 6 undergoes greater wear at low sliding speed needs further investigation. One possibility is that early during wear, oxide transferred from the Stellite 6 was embedded in the Nimonic 80A surface, creating a composite structure that with continued sliding enhanced wear and oxide debris generation from the Stellite 6. Similar behaviour has been observed during wear of some steels by softer copper-based materials [35].

Once the debris was generated and transferred to the Nimonic 80A surface, the oxide particles remained loose at room temperature to 390^{o}C and did not develop into 'glaze'. The abrasive nature of these oxides promoted further wear of, particularly, the Stellite 6 surface; however, the debris also eliminated metal-to-metal contact and wear levels remained low. Another important observation is the enhanced wear of Stellite 6 at 510°C to 750^{o}C, leading to the generation of oxide debris and subsequent transfer to the Nimonic 80A surface; this facilitated rapid formation and sustainment of the 'glaze', as demonstrated by the friction data (Fig. 4), where steady state sliding was sustained without any significant jumps to indicate 'glaze-layer' break-up. In this context, two issues are important. Firstly, preferential oxidation of Co and Cr is indicated by ΔG values in Table 2. The second relevant issue is the hexagonal-close-packed to face-centred-cubic phase transformation in

Stellite 6. Although Cr increases the transformation temperature by ~150°C, to ~900°C [36], the interfacial temperature generated by ambient and frictional heating and asperity interaction may be sufficient to cause the interfacial temperature to reach this level. Also, other alloying elements may lower the transition temperature for this phase change. The formation of a face-centred-cubic phase in Stellite 6, at least at the highest sliding temperatures, will lead to easier (easy dislocation slip) deformation and more material removal.

Oxide	$\Delta G_{727°C}$ (kJ.mol^{-1})
$Co + ½O_2 \rightleftharpoons CoO$	-163.3
$3Co + 2O_2 \rightleftharpoons Co_3O_4$	-525.0
$2Cr + 1½O_2 \rightleftharpoons Cr_2O_3$	-861.6
$Ni + ½O_2 \rightleftharpoons NiO$	-150.7

Table 2: Free energies of formation for key oxides (Co, Cr and Ni) at 727°C under conditions of static oxidation [36]

4.2 Sliding at 0.654 m.s^{-1} and 0.905 m.s^{-1}

At the higher sliding speeds the wear behaviour was different to that observed at 0.314 m.s^{-1}.

At room temperature and 270°C, wear was confined to the Stellite 6 surface. The loose, generated $CoCr_2O_4$ / Co_3O_4 debris did not develop into a 'glaze'. Instead, it underwent deformation and spreading on the Nimonic 80A surface, especially at 270°C, where it largely prevented metal-to-metal wear. Thus the debris was responsible for the low wear rate observed at room temperature and 270°C.

The failure of the debris to undergo sintering required for formation of 'glaze' was due to its low residence time between the wear surfaces. Agglomeration and sintering also require the particles to maintain their shape, to minimise their surface energy at the in-contact points. The deformed particles failed to satisfy this condition.

The effects of lower residency, higher ejection rates and loss of debris shape integrity were demonstrated at 390°C by the difference in behaviour at the two speeds. At 0.654 m.s^{-1}, increased debris retention allowed the loose $CoCr_2O_4$ / Co_3O_4 debris to continue to separate the sample and counterface surfaces, and low wear was observed. However, at 0.905 m.s^{-1},

the lower residency coupled with more debris deformation (due to a combination of greater mechanical action and higher localised temperatures) allowed metal-to-metal contact and severe wear. At 450°C, where the debris was no longer able to prevent metal-to-metal contact, even at 0.654 $m.s^{-1}$, the transition to severe wear now also occurred at that speed.

It has been suggested that this change to severe wear is due to decreases in strength for Nimonic 80A and phase changes in the Stellite 6 on increasing the test temperature [6]. However, Nimonic 80A retains its strength (~600 MPa) up to ~600°C [37], thus, loss of strength is unlikely to significantly contribute to the severe wear transition. Also, as the phase transformation temperature for Stellite 6 is ~900°C [36], enhanced removal from the Stellite 6 due to this transformation is unlikely to be a major factor in the wear transition (even accounting for frictional heating, asperity interactions and minor alloying additions). Thus, it is the increased deformation of the oxide debris and its failure to prevent metal-to-metal contact in low debris residency conditions that leads to the transition to severe wear.

The severe wear mechanism also dominated at 510°C. The significant metal-to-metal wear of the Nimonic 80A surface accompanied by the production of large, flat, predominantly Nimonic 80A wear debris, indicates a delamination type of wear mechanism. Both wear surfaces (Figs. 6 and 8) were completely devoid of debris; although increasing temperature increases the rate of oxidation, no 'glaze' formation occurred, due mainly to the low retention and low residence time of debris on the wear surfaces. In the absence of 'glaze', a classic high friction metal-to-metal contact scenario occurs, with wear on the softer Nimonic 80A, probably aided by Ni and Cr oxides (although none were detected) at 510°C.

Severe wear continued at 570°C and 630°C, despite the generation of increasing amounts of NiO and Cr_2O_3 particularly at 630°C. Oxide generation was enhanced by greater mechanical action and frictional heating, resulting in more debris at the higher speed. However, contact was still metal-to-metal, with continued production of large, flat, metallic debris, indicating a delamination type mechanism. The appearance of the oxide debris was accompanied by continued increases in wear at 0.654 $m.s^{-1}$, but not at 0.905 $m.s^{-1}$ (Fig. 5), despite the absence of a clear change in wear mechanism from severe wear. However, the greater amounts of oxide produced at 0.905 $m.s^{-1}$ may, to a limited degree, impede direct metal-to-metal contact, while the lower amounts produced at 0.654 $m.s^{-1}$, insufficient to significantly impede metal-to-metal contact, may have continued to contribute as wear levels reached a maximum at 630°C (Fig. 5); this combination of severe wear and oxide abrasion appears to be most effective for removing material from the Nimonic 80A surface.

A further change in the wear mechanism occurred at 690°C, due to further increases in NiO and Cr_2O_3 generation. Here, the rate of formation of the oxide debris was sufficient to exceed the rate of debris elimination by ejection from the wear surfaces. Consequently, debris residency was high enough to eliminate metal-to-metal contact, resulting in a technically mild wear regime (although wear levels remained high) reflected by lower friction values (Fig. 7). The NiO and Cr_2O_3 debris did not form 'glaze' on the Nimonic 80A surface, as they have a very low tendency to sinter and thus form 'glaze' layers, but instead contributed to wear by abrasion. The abrasive action resulted in fine parallel wear groves on the worn Nimonic 80A surface at 690°C and 750°C (Figs. 5 and 6).

The more pronounced oxide generation and greater amounts of oxide debris at 0.905 $m.s^{-1}$ than at 0.654 $m.s^{-1}$, leading to oxide build-up in a few areas on the Nimonic 80A surfaces, can be attributed to greater mechanical action and frictional heating. However, these isolated areas of oxide build-up did not fully develop into clear compacted oxide or 'glaze' layers and had little effect on the amounts of wear. The rate of debris removal and breakdown at 0.905 $m.s^{-1}$ was easily sufficient to overcome the accumulation and development of these isolated areas and the poor sintering characteristics of the NiO and Cr_2O_3 debris, necessary to form 'glaze'.

The reasons for the inability of the debris generated from the Nimonic 80A to form 'glaze' layers, are dealt with in more detail elsewhere [1,4]. However, it is suggested that Cr_2O_3 inhibits the sintering process and, thus, promotes wear by abrasion rather than the formation of a protective oxide 'glaze'. Sliding of Cr-free Nickel 200™ against Stellite 6 under high speed, high-temperature conditions [1], resulted in the formation of NiO debris that readily formed a wear protective 'glaze' on both sample and counterface. Also, at 0.314 $m.s^{-1}$, Cr quite readily formed 'glaze' in combination with Co from the Stellite 6 ($CoCr_2O_4$ / Co_3O_4) that significantly reduced wear. Thus, it is suggested that the composition and phase of the oxide can have a significant affect on its 'glaze' forming abilities.

The apparently poor sintering and 'glaze' forming characteristics of NiO and Cr_2O_3 generated from Nimonic 80A at first seems to contradict the extensive studies carried out into 'glaze' formation with Nimonic 80A-based systems [15, 17-21]; however, they were conducted using lower sliding speeds with a pin-on-disk configuration. Such systems also have a higher degree of debris retention, which provides greater opportunity for the oxide debris to sinter together to form 'glaze' layers. The present 'block-on-cylinder' configuration is a unidirectional sliding wear system that promotes debris mobility and

ejection over retention, especially at higher sliding speeds. The decreased residency and greater mobility of the debris do not allow sufficient contact time between debris particles for sintering and welding processes to occur, as necessary for 'glaze' formation.

The development of the limited 'glaze' layers on the Stellite 6 counterface protected it from high levels of wear, with only a brief period of metal-to-metal wear before the 'glaze' layer formed (Fig. 7). This further supports the observation that the oxide debris generated at 750°C acts as an abrasive, enhancing the wear of the Nimonic 80A. The limited 'glaze' layer also seals off the Stellite 6 surface, so carbides present in the surface cannot assist removal of material from the Nimonic 80A by ploughing, as has been suggested elsewhere [6]. It has also been demonstrated elsewhere that the carbides are not sufficiently hard enough to disrupt 'glaze' formation and enhance wear [1].

There are two observations during this study that cannot be properly explained at this stage. Firstly, the switch from greater wear of the Stellite 6 at 0.314 $m.s^{-1}$ to greater wear of the Nimonic 80A at 0.654 $m.s^{-1}$ and 0.905 $m.s^{-1}$ cannot be attributed to the 'block-on-cylinder' geometry favouring wear of either the Nimonic 80A sample or the Stellite 6 counterface depending on sliding speed. On reversal of the sample and counterface during studies under identical conditions [1], Stellite 6 still underwent greater wear at 0.314 $m.s^{-1}$ and Nimonic 80A suffered greater damage at 0.905 $m.s^{-1}$. Secondly, it is not clear why NiO and Cr_2O_3 formation from the Nimonic 80A is favoured over $CoCr_2O_4$ / Co_3O_4 formation from the Stellite 6 at 0.654 $m.s^{-1}$ and 0.905 $m.s^{-1}$ at the higher temperatures, as the ΔG values (Table 2) suggest that preferential development of Co-containing oxides should be the case.

5. Wear Map for Nimonic 80A versus Stellite 6

If the data from the current test program are compared with respect to sliding speed and temperature, it is possible to set up a wear map describing the wear behaviour as a function of these variables, as shown in Fig. 9. However, the map has a number of weaknesses that need to be resolved to provide a fuller picture of wear for Nimonic 80A versus Stellite 6 and to identify with greater accuracy, the boundaries between the various types of wear. It is necessary to carry out sliding wear at a greater number of temperatures and sliding speeds, since the map can only define a given form of wear to within the nearest 60ºC (the difference between each test temperature) or ~1/3 $m.s^{-1}$ sliding speed.

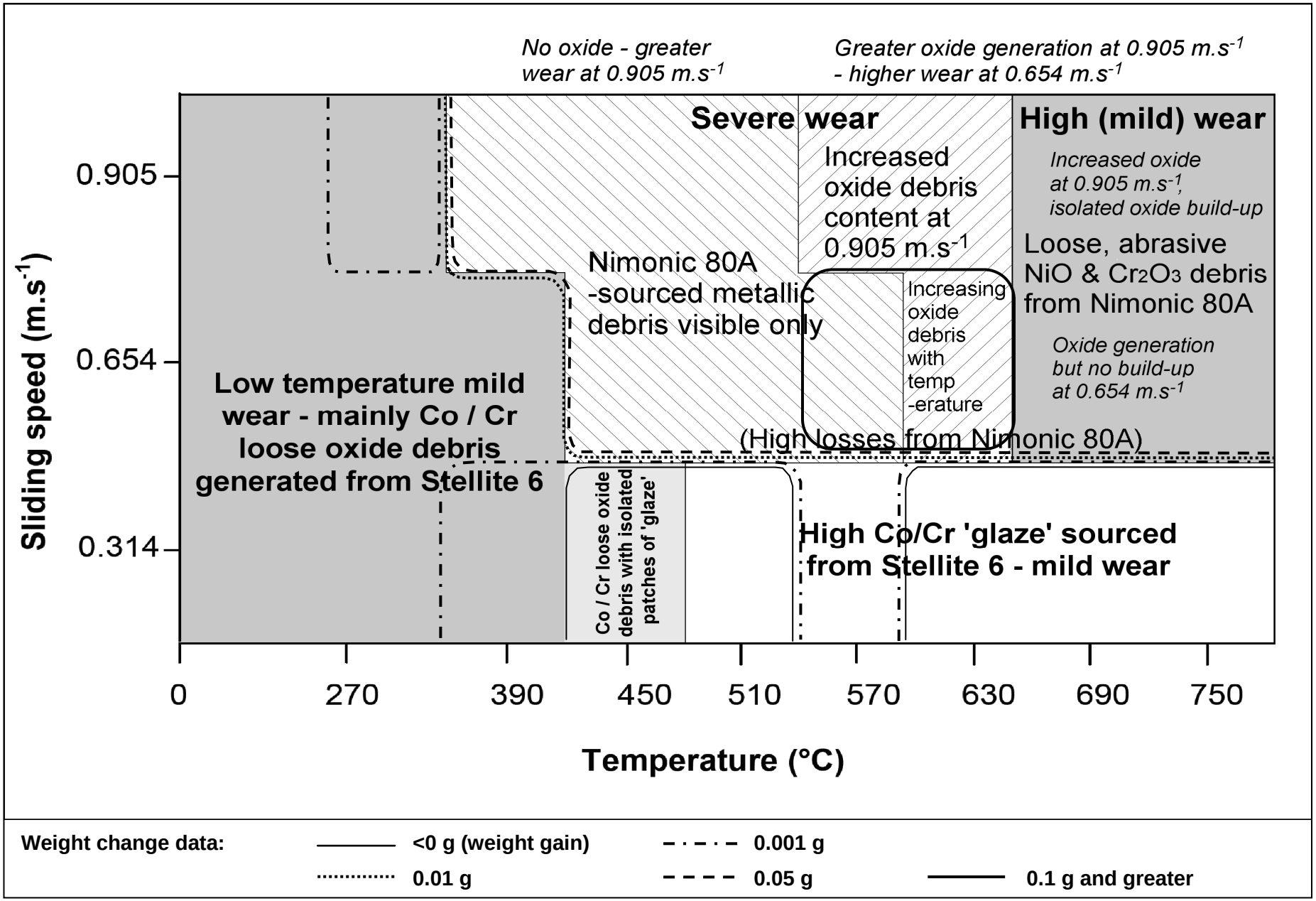

Fig. 9: Wear map for Nimonic 80A versus Stellite 6 (load 7N, sliding distance 4,522 m), with weight loss (contour) data superimposed

6. Summary of Results

The following behaviour was observed at 0.314 $m.s^{-1}$:

- A low temperature mild wear regime existed between room temperature and 450°C, with the wear surfaces separated by a layer of discrete Co-Cr oxide particles (i.e. loose debris), primarily from the Stellite 6. Increased agglomeration and sintering of the debris was observed at 390°C, with isolated patches of 'glaze' at 450°C (although most of the oxide remained as loose debris).
- Mild wear persisted between 510°C and 750°C, with the oxide sintering to form comprehensive 'glaze' layers. The primary source of debris was again the Stellite 6.

The following behaviour was observed at 0.654 $m.s^{-1}$:

- A low temperature mild wear regime existed between room temperature and 390°C, with a layer of discrete Co-Cr oxide particles, sourced primarily from the Stellite 6, separating the wear surfaces.
- Severe wear due to direct metal-to-metal contact between sample and counterface dominated between 450°C and 630°C. No oxide was observed between 450°C and 570°C; however, limited amounts of Ni and Cr oxides were evident at 630°C, although were insufficient to impede metal-to-metal contact and may instead have assisted wear at 630°C.
- A mild wear regime was evident at 690°C and 750°C. Although this was technically a mild wear regime with oxidational wear, Nimonic 80A wear levels remained high due to abrasion by large amounts of Ni and Cr oxides (displaying poor sintering characteristics) sourced from the Nimonic 80A (the material removed then became the abrasive agent); no clear evidence of compacted oxide or 'glaze' formation was observed on the Nimonic 80A surface. A limited patchy high Ni-Cr oxide 'glaze' layer was present only on the Stellite 6 counterface.

The following behaviour was observed at 0.905 $m.s^{-1}$:

- Low temperature mild wear occurred only at room temperature and 270°C, with wear surfaces again separated by discrete Co-Cr oxide particles; the main source of debris was the Stellite 6.
- Severe wear due to direct metal-to-metal contact dominated between 390°C and 630°C. No oxide was observed between 390°C and 510°C, but at 570°C and especially 630°C, increasing amounts of Ni and Cr oxides were observed. The production of this oxide

was sufficient to decrease metal-to-metal contact (although not to eliminate severe wear).

- A mild wear regime was observed at 690°C and 750°C. As at 0.654 $m.s^{-1}$, this is technically a mild wear regime with oxidational wear; however, high losses from the Nimonic 80A were observed, due to abrasion by large amounts of Nimonic 80A-sourced oxides. These Ni and Cr oxides showed poor sintering characteristics and there were only limited, isolated build-ups of oxide on the Nimonic 80A that failed to develop into comprehensive compacted oxide or 'glaze' layers. However, wear at 0.905 $m.s^{-1}$ was lower than at 0.654 $m.s^{-1}$, at 690°C and 750°C; this was attributed to more effective separation of sample and counterface by the increased presence of oxide debris at the sliding interface. A rough patchy Ni-Cr oxide 'glaze' layer was again evident only on the Stellite 6 counterface.

References

[1] I.A. Inman, Ph.D. Thesis "Compacted Oxide Layer Formation under Conditions of Limited Debris Retention at the Wear Interface during High Temperature Sliding Wear of Superalloys", Northumbria University, UK (2003).

[2] I. A. Inman, S. Datta, H.L. Du, J.S. Burnell-Gray, S. Pierzgalski, Q. Luo, "Microscopy of 'glazed' layers formed during high temperature sliding wear at 750°C", Wear 254 (2003) 461-467.

[3] S. Datta, I. Inman, H.L. Du, Q. Luo, "Microscopy of 'glazed' layers formed during high temperature wear, Invited Talk at the Institute of Materials", Tribology Meeting, London, November 2001.

[4] I.A. Inman, S. Datta, H.L. Du, J.S. Burnell-Gray, S. Pierzgalski and Q. Luo "Studies of High Temperature Sliding Wear of Metallic Dissimilar Interfaces", Trib. Int. (2005), *article in press*.

[5] P .D. Wood, Ph.D. Thesis "The Effect of the Counterface on the Wear Resistance of Certain Alloys at Room Temperature and 750°C", Northumbria University, UK (1997).

[6] S. Rose, Ph.D. Thesis "Studies of the High Temperature Tribological Behaviour of Some Superalloys", Northumbria University, UK (2000).

[7] F.H. Stott, D.S. Lin, G.C. Wood, "The structure and mechanism of formation of the "glaze" oxide layers produced on nickel-based alloys during wear at high temperatures", Corrosion Science 13 (1973) 449 - 469.

[8] M. Johnson, P. Moorhouse, J.R. Nicholls, DTI Industry Valve Project, 61-68 (1990).

[9] J-N. Aoh, J-C. Chen, "On the wear characteristics of cobalt-based hardfacing layer after thermal fatigue and oxidation", Wear 250-251 (2001) 611.

[10] Singh, J. and Alpas, A.T., "High-temperature Wear and Deformation Processes in Metal Matrix Composites," Metallurgical and Materials Transactions A, 27 (1996) 3135-3148

[11] F.H. Stott, J. Glascott, G.C. Wood, “Factors affecting the progressive development of wear-protective oxides on iron-base alloys during sliding at elevated temperatures”, Wear 97 (1984) 93-106.

[12] M.G. Gee, N.M. Jennett, “High resolution characterisation of tribochemical films on alumina”, Wear 193 (1995) 133-145.

[13] P.D. Wood, P.K. Datta, J.S. Burnell-Gray, N. Wood, “Investigation into the high temperature wear properties of alloys contacting against different counterfaces, Materials Science Forum”, 251-254 (1997) 467-474.

[14] Wisbey, C.M. Ward-Close, Materials Science and Technology, “Wear resistant surfaces on high temperature titanium alloy and titanium aluminide by diffusion bonding”, 13 (1997) 349-355.

[15] J. Jiang, F.H. Stott, M.M. Stack, ”The effect of partial pressure of oxygen on the tribological behaviour of a nickel-based alloy, N80A, at elevated temperatures”, Wear 203-204 (1997) 615-625.

[16] X.Y. Li, K.N. Tandon, “Microstructural characterization of mechanically mixed layer and wear debris in sliding wear of an Al alloy and an Al based composite”, Wear 245 (2000) 148-161.

[17] J. Jiang, F. H. Stott, M. M. Stack, “A generic model for dry sliding wear of metals at elevated temperatures” Wear 256 (2004) 973-985.

[18] J. Jiang, F. H. Stott, M. M. Stack, “The role of triboparticulates in dry sliding wear” Trib. Int. 31-5 (1998) 245-256.

[19] J. Jiang, F. H. Stott, M. M. Stack, “Characterization of wear scar surfaces using combined three-dimensional topographic analysis and contact resistance measurements” Trib. Int. 30-7 (1997) 517-526.

[20] J. Jiang , F. H. Stott, M. M. Stack, “A mathematical model for sliding wear of metals at elevated temperatures” Wear 181-183 (1995) 20-31.

[21] J. Jiang, F. H. Stott, M. M. Stack, “Some frictional features associated with the sliding wear of the nickel-base alloy N80A at temperatures to 250 °C” Wear 176 (1994) 185-194.

[22] J.K. Lancaster “The Formation of Surface Films at the Transition Between Mild and Severe Metallic Wear”, Proc. Royal Society London, A 273 (1962) 466-483

[23] N.C. Welsh “The Dry Wear of Steels 1, the General Pattern of Behaviour” Phil. Trans., 257A (1965) 31-50

[24] N.C. Welsh “The Dry Wear of Steels 2, Interpretation and Special Features” Phil. Trans., 257A (1965) 51-70

[25] C. Subramanium “Wear of Al-12.3 Wt% Si Alloy Slid Against Various Counterface Materials” Scripta Metallurgica 25 (1991) 1369-1374

[26] P.J. Blau “Mechanisms for Traditional Friction and Wear Behaviour of Sliding Metals” Wear 72 (1981) 55-66

[27] H. So “Characteristics of Wear Results Tested by Pin-on-Disc at Moderate to High Speeds”, Tribo. Int., Vol. 25, No. 5 (1996) 415-423

[28] H. So “Wear Behaviours of Laser-Clad Stellite Alloy 6”, Wear 192 (1996) 78-84

[29] S.C. Lim “Recent Development in Wear Maps”, Tribo. Int., Vol. 31, Nos. 1-3 (1998) 87-97

[30] S.C. Lim “The relevance of wear-mechanism maps to mild-oxidational wear”, Tribo. Int., Vol. 35, No. 11 (2002) 717-723

[31] T.H.C. Childs “The Sliding Wear Mechanisms of Metals, Mainly Steels”, Tribo. Int., 13 (1980) 285-293

[32] K. Kato and K. Hokkirigawa “Abrasive Wear Diagram”, Proc. Eurotrib ’85, Vol. 4, Section 5.3, Elsevier, Amsterdam (1985) 1-5

[33] B.V. Cockeram “The Fracture Toughness and Toughening Mechanisms of Nickel-Base Wear Materials” Metallurgical and Materials Transactions A, 33A (2002) 33-57

[34] B.V. Cockeram “Some Observations of the Influence of d-Ferrite Content on the Hardness, Galling Resistance, and Fracture Toughness of Selected Commercially Available Alloys” Metallurgical and Materials Transactions A, 33A (2002) 3403-3419

[35] W Czupryk “Frictional Transfer of Iron in Oxidative Wear Conditions during Lubricated Sliding”, Wear 237 (2000) 288-294

[36] E.A. Brandes and G.B. Brook “Smithells Metals Reference Book: Seventh Edition”, Butterworth Heinemann (1992)

[37] G. Fisher, Unpublished Work, Northumbria University (1998)

Errata

Table 1 (Page 3): In the title, ‘Nominal compositions of alloys (at%)’ should read ‘Nominal compositions of alloys (wt%)’.